Structural Engineering and Mechanics, Vol. 8, No. 3 (1999) 233-242
DOI: http://dx.doi.org/10.12989/sem.1999.8.3.233

A finite strip method for elasto-plastic analysis of thin-walled structures under pure bending

M.S. Cheung †

Department of Civil Engineering, University of Ottawa, Ottawa, Ontario, K1N 9B4, Canada

G. Akhras ‡

Department of Civil Engineering, Royal Military College of Canada, Kingston, Ontario, K7K 5L0, Canada

W. Li ‡†

Department of Civil Engineering, Carleton University, Ottawa, Ontario, K1S 5B6, Canada

Abstract. In the present study, the elasto-plastic analysis of prismatic plate structures subjected to pure bending is carried out using the finite strip method. The end cross-sections of the structure are assumed to remain plane during deformation, and the compatibility along corner lines is ensured by choosing proper displacement functions. The effects of both the initial geometrical imperfections and residual stresses due to fabrication are included in the combined geometrically and materially nonlinear simulation. The von-Mises yield criterion and the Prandtl-Reuss flow theory of plasticity are applied in modelling the elasto-plastic behavior of material. Newton-Raphson iterations are carried out as the rotation of the end cross sections of the structure is increased step by step. The parameter representing the overall axial strain of structure is adjusted constantly during the iteration process in order to eliminate the resulting overall axial force on any cross-section of the structure in correspondence with the assumption of zero axial force in pure bending. Several numerical examples are presented to validate the present method and to investigate the effects of some material and geometrical parameters.

Key words: finite strip; elasto-plastic analysis; thin walled structures; pure bending.

1. Introduction

Some thin-walled structures are subjected to severe flexural loading, which can be simplified as pure bending. Under such loading, the structures undergo combined local buckling, overall buckling and elasto-plastic deformation. The ultimate strength and the inelastic post-buckling behavior are very important issues for design and development of such structures. Therefore, creation of more accurate and more efficient numerical method to model this behavior is of

† Adjunct Professor
‡ Professor
‡† Research Engineer

practical interest.

Finite element method has been applied to this problem since two decades ago (Zienkiewicz 1977). However, for the prismatic plate structures, or those which can be reasonably idealized as such structures, the finite strip method has advantages over the former method with significant computational saving (Cheung *et al.* 1996). The finite strip method has been successfully employed to simulate the nonlinear post-buckling behavior of plate structures under longitudinal compression (e.g., Hancock 1981, Sridharan and Graves-Smith 1981 and Guo and Lindner 1993) and has shown its satisfactory performance.

In the present study, the finite strip method is extended to the elasto-plastic analysis of prismatic plate structures subjected to pure bending. The end cross-sections of the structure are assumed to remain plane during deformation, and the compatibility along corner lines is ensured by choosing proper displacement functions. The effects of the initial geometrical imperfections and residual stresses due to fabrication are included in the combined geometrically and materially nonlinear simulation. The von-Mises yield criterion and the Prandtl-Reuss flow theory of plasticity are employed in modelling the elasto-plastic behavior of the material. The Newton-Raphson iteration is carried out as the rotation of the end cross sections of the structure is increased step by step. The parameter representing the overall axial strain of the structure is adjusted constantly during the solution process in order to eliminate the resulting overall axial force on any cross-section of the structure in compliance with the assumption of zero axial force in pure bending.

Several numerical examples are presented to validate the present method and to investigate the effects of some material and geometrical parameters.

2. Displacement functions

In the present analysis, the thin-walled structure (Fig. 1) is modeled by a number of finite strips, each of which has three equally spaced nodal lines (Fig. 2). In the transverse direction of the strip, quadratic interpolation is used for in-plane deformation whilst Hermitian cubic polynomials are employed for out-of-plane bending. The strip is hinged at both ends, and the end cross-sections are assumed to remain plane during deformation. Moreover, the displacements of two adjacent strips along any corner line of the structure must be compatible. These conditions can be satisfied

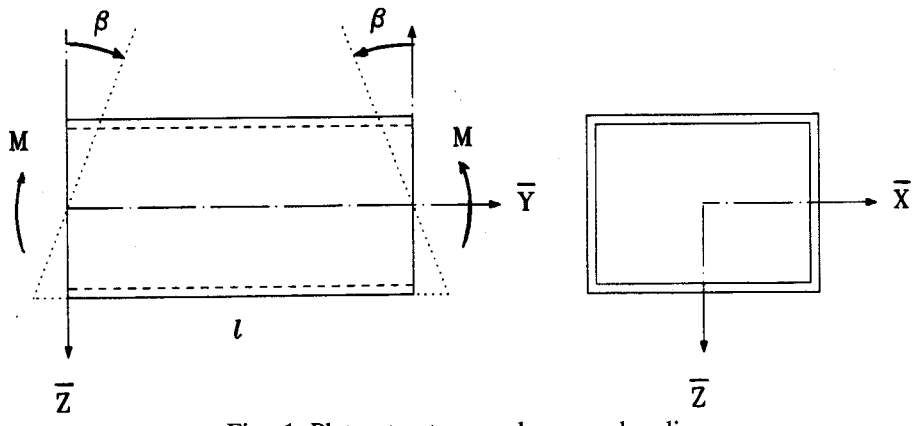

Fig. 1 Plate structure under pure bending

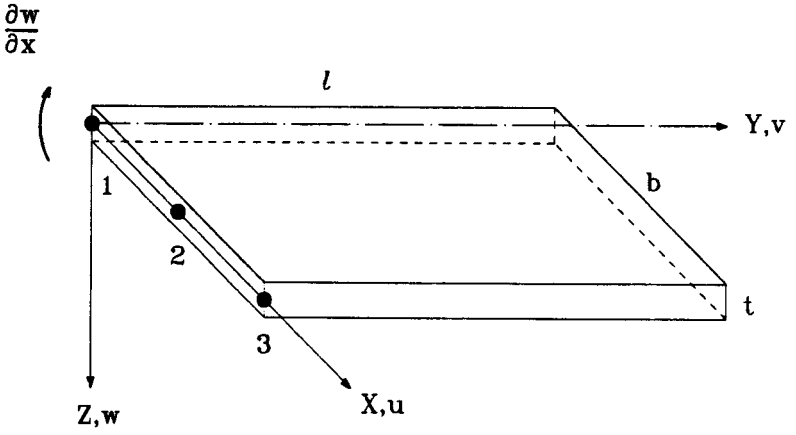

Fig. 2 A finite strip

by the following displacement functions:

$$u = \sum_{m=1}^{r} \sum_{i=1}^{3} N_i(x) u_{im} \sin\frac{m\pi y}{l}$$

$$v = \sum_{m=1}^{r} \sum_{i=1}^{3} N_i(x) v_{im} \sin\frac{(m+1)\pi y}{l} + \beta\bar{z}\left(\frac{2y}{l} - 1\right) + \alpha y$$

$$w = \sum_{m=1}^{r} \sum_{i=1,3} [F_i(x) w_{im} + H_i(x)\left(\frac{\partial w}{\partial x}\right)_{im}] \sin\frac{m\pi y}{l} \tag{1}$$

where u and v are the in-plane displacements of the point (x, y, 0) on the midplane, w is the deflection which is assumed to be constant in the thickness direction z; r is the number of harmonics employed in the analysis; u_{im}, v_{im}, w_{im} and $(\partial w/\partial x)_{im}$ are the displacement parameters for the i-th nodal line and the m-th harmonic; l is the length of the strip; $N_i(x)$ is the quadratic interpolation function for nodal line i (i=1 to 3) with the following expression:

$$N_i(x) = \prod_{\substack{j=1 \\ j\neq i}}^{3} \frac{x - x_j}{x_i - x_j} \tag{2}$$

$F_i(x)$ and $H_i(x)$ (i=1, 3) are Hermitian cubic polynomials as below:

$$F_1(x) = 1 - 3(\frac{x}{b})^2 + 2(\frac{x}{b})^3$$

$$F_3(x) = 3(\frac{x}{b})^2 - 2(\frac{x}{b})^3$$

$$H_1(x) = x[1 - 2\frac{x}{b} + (\frac{x}{b})^2]$$

$$H_3(x) = x[(\frac{x}{b})^2 - \frac{x}{b}] \tag{3}$$

in which b is the width of the strip; β is the rotation of each end cross-section (Fig. 1), its value is given as external load; $\bar{z}$ is the global vertical coordinate with the origin located on the elastic neutral axis of structural cross-section; α is the longitudinal strain due to global elongation of the structure at level $\bar{z}$=0. Its value is assumed to be zero initially and is adjusted constantly during

iteration to eliminate the axial force of the structure as mentioned later.

3. Strains and stresses

Including the effects of initial geometrical imperfections u_o and w_o, the following strain-displacement relationships are used in the present analysis:

$$\varepsilon_x = \bar{\varepsilon}_x - z\frac{\partial^2(w-w_o)}{\partial x^2}$$

$$\varepsilon_y = \bar{\varepsilon}_y - z\frac{\partial^2(w-w_o)}{\partial y^2}$$

$$\gamma_{xy} = \bar{\gamma}_{xy} - 2z\frac{\partial^2(w-w_o)}{\partial x\,\partial y} \tag{4}$$

where $\bar{\varepsilon}_x$, $\bar{\varepsilon}_y$ and $\bar{\gamma}_{xy}$ are the strains of the midplane and are defined as

$$\bar{\varepsilon}_x = \frac{\partial(u-u_o)}{\partial x} + \frac{1}{2}[(\frac{\partial w}{\partial x})^2 - (\frac{\partial w_o}{\partial x})^2]$$

$$\bar{\varepsilon}_y = \frac{\partial v}{\partial y} + \frac{1}{2}[(\frac{\partial w}{\partial y})^2 - (\frac{\partial w_o}{\partial y})^2] + \underline{\frac{1}{2}[(\frac{\partial u}{\partial y})^2 - (\frac{\partial u_o}{\partial y})^2]}$$

$$\bar{\gamma}_{xy} = \frac{\partial(u-u_o)}{\partial y} + \frac{\partial v}{\partial x} + [\frac{\partial w}{\partial x}\frac{\partial w}{\partial y} - \frac{\partial w_o}{\partial x}\frac{\partial w_o}{\partial y}] \tag{5}$$

The underlined term in the expression of $\bar{\varepsilon}_y$ accounts for the nonlinear effect of membrane displacement. The other nonlinear terms are considered to be of secondary importance and have been neglected in the above equations.

In the elastic stage, the linear stress-strain relationships hold:

$$\begin{Bmatrix}\sigma_x\\ \sigma_y\\ \tau_{xy}\end{Bmatrix} = \frac{E}{1-\nu^2}\begin{bmatrix}1 & \nu & \\ \nu & 1 & \\ & & \frac{1-\nu}{2}\end{bmatrix}\begin{Bmatrix}\varepsilon_x\\ \varepsilon_y\\ \gamma_{xy}\end{Bmatrix} + \begin{Bmatrix}\sigma_{xo}\\ \sigma_{yo}\\ \tau_{xyo}\end{Bmatrix} \tag{6}$$

or in a compact form

$$\{\sigma\} = [D]\{\varepsilon\} + \{\sigma_o\} \tag{7}$$

where E is Young's modulus, ν is Poisson's ratio; σ_{xo}, σ_{yo} and τ_{xyo} represent the initial residual stresses due to fabrication.

According to the von-Mises criterion, the material yields when the equivalent stress $\bar{\sigma}$ reaches the uniaxial yield stress σ_Y:

$$\bar{\sigma} = \sqrt{\sigma_x^2 + \sigma_y^2 - \sigma_x\sigma_y + 3\tau_{xy}^2} = \sigma_Y \tag{8}$$

After yielding, the stresses can be calculated using the incremental stress-strain relationship:

$$d\{\sigma\} = [D]_{ep}\, d\{\varepsilon\} = [D]\, d\{\varepsilon\} - [C]\, d\{\varepsilon\} \tag{9}$$

where $[D]_{ep}=[D]-[C]$ is the elasto-plastic matrix, which can be formed from the current stress level according to the Prandtl-Reuss flow theory of plasticity. The related theoretical foundation has been described in details in many references (e.g., Zienkiewicz 1977, Owen and Hinton 1980) and is not to be repeated here. In the present analysis, the following procedures are used for elastic-perfectly plastic material after yielding:

First, only the elastic part of the stress increments $[D]d\{\varepsilon\}$ is added to the stresses obtained in the previous loading step:

$$\{\sigma\}_e = \{\sigma\}^k + [D](\{\varepsilon\} - \{\varepsilon\}^k) \tag{10}$$

where $\{\varepsilon\}$ is the current value of the strain vector, $\{\sigma\}^k$ and $\{\varepsilon\}^k$ are respectively the last values of the stress and strain vectors in the previous loading step k.

Then, the equivalent stress $\bar{\sigma}_e$ of $\{\sigma\}_e$ is calculated using (8). If $\bar{\sigma}_e < \sigma_Y$, unloading occurs in the region under consideration, and the elastic relationship should be used. Therefore, the current stress vector is

$$\{\sigma\} = \{\sigma\}_e \tag{11}$$

Otherwise with $\bar{\sigma}_e \geq \sigma_Y$ the plastic deformation occurs and then Eq. (9) stands. Thus, the second part of the stress increments in Eq. (9) must be included:

$$\{\sigma\} = \{\sigma\}_e - [C](\{\varepsilon\} - \{\varepsilon\}^k) \tag{12}$$

where

$$[C] = \frac{E}{Q(1-\nu^2)} \begin{bmatrix} (S_1 + \nu S_2)^2 & & \text{Symm.} \\ (S_1 + \nu S_2)(S_2 + \nu S_1) & (S_2 + \nu S_1)^2 & \\ (S_1 + \nu S_2)S_3 & (S_2 + \nu S_1)S_3 & S_3^2 \end{bmatrix} \tag{13}$$

in which

$$S_1 = \sigma_x^k - (\sigma_x^k + \sigma_y^k)/3$$
$$S_2 = \sigma_y^k - (\sigma_x^k + \sigma_y^k)/3$$
$$S_3 = (1-\nu)\,\tau_{xy}^k$$
$$Q = S_1^2 + S_2^2 + 2\nu S_1 S_2 + 2S_3^2/(1-\nu)$$

and the superscript k represents the previous loading step.

The stresses obtained from Eq. (12) should be brought to yield surface in order to reduce numerical error:

$$\{\sigma\}_{new} = \frac{\sigma_Y}{\bar{\sigma}}\{\sigma\} \tag{14}$$

where $\bar{\sigma}$ is the equivalent stress of $\{\sigma\}$.

4. Solution procedure

The entire loading process is carried out in a number of steps. In each step, the end rotation β

of the structure is increased by a specified amount, and the Newton-Raphson iterations are implemented until convergence occurs.

Each finite strip is divided into several layers through the thickness direction. In each iteration, the strains and stresses are computed at the level of each layer. And then, the tangential stiffness matrix and the vector of unequilibrium loads (Cheung *et al.* 1996) are updated. The value of α is assumed to be zero initially with the origin of $\bar{z}$ located on the elastic neutral axis. Afterwards, its value is modified according to the resulting average axial force and average axial stiffness of the structure in each iteration:

$$\alpha^{n+1} = \alpha^n - \frac{\int_V \sigma_y \, dxdydz}{\int_V D_{ep22} \, dxdydz} \tag{15}$$

where V denotes the volume of entire structure; n is the sequential number of iteration; D_{ep22} is the second diagonal item of $[D]_{ep}$ (see Eq. (9)) and is defined as

$$D_{ep22} = \begin{cases} \dfrac{E}{1-\nu^2} & \text{for elastic region} \\ \dfrac{E}{1-\nu^2} - C_{22} & \text{for plastic region} \end{cases} \tag{16}$$

where C_{22} is the item of $[C]$ given in Eq. (13).

Thus, the axial force at any cross-section of the structure is reduced to a minimum in compliance with the assumption of zero axial force in pure bending.

Based on the updated value of α, the stress σ_y can be recalculated. Then, the bending moment on any cross-section of the structure is obtained as

$$M = \frac{1}{l} \int_V \sigma_y \bar{z} \, dxdydz \tag{17}$$

in which l is the length of the structure, M is the average value of the bending moment over the length of the structure and $\bar{z}$ is the structural vertical coordinate. The location of the origin of $\bar{z}$ has negligible influence on the value of M since the axial force is zero.

5. Numerical examples

5.1. Simply supported rectangular plate under axial compression

A rectangular plate is simply supported on its four edges. The thickness of the plate is t, the width is a=55t and the aspect ratio is a/l=0.875. The material properties are Young's modulus E= 200,000MPa, Poisson's ratio ν=0.3 and the uniaxial yield stress σ_Y=250MPa. The end cross-sections move rigidly under uniform compressive displacement, whilst the unloaded edges are free to pull in. The initial geometrical imperfection has a pattern of

$$w_o = 0.005a \sin\frac{\pi x}{a} \sin\frac{\pi y}{l}$$

The plate is analyzed using the present method by assuming β=0 and taking $-\alpha$ as the external loading, namely the compression strain ε. Taking advantage of symmetry, half the plate is divided into four strips with three layers each, and only two symmetrical series terms (m=1, 3) are used in the analysis. The edge strip is of $3t$ width with a residual stress $\sigma_{yo}=\sigma_Y$, while the other three strips are of equal width over the rest of the model with a residual stress $\sigma_{yo}=-(3t/0.5a\text{-}3t)\,\sigma_Y$, which means that the resultant of the residual stress σ_{yo} on the cross-section of the plate is zero. Further refining the model only yields little improvement.

The resulting compression force P vs the longitudinal strain ε is plotted in Fig. 3 in comparison with the finite difference solution of Harding *et al.* (1977) and the spline finite strip solution of Guo *et al.* (1993). In this figure $P_Y=(at/2)\sigma_Y$, $\varepsilon_Y=\sigma_Y/E$. It can be seen that the agreement between the present and existing results is generally good.

Because the deformation pattern of a plate under compression is similar to that of the top flange of a thin-walled structure under pure bending, and the combined geometrical and material nonlinear deformation of the top flange is the major contribution to the nonlinearity of the latter structure, the present example can be reasonably used to validate the present approach.

5.2. Box beam under pure bending

A box beam of length l=100.0 cm is subjected to pure bending as shown in Fig. 1. All plate components have an identical thickness t=1.0 cm and a width a=55.0 cm. The material properties are E=200,000MPa, ν=0.3 and σ_Y=320MPa. The initial geometrical imperfections have the following pattern

$$w_o = 0.005a \sin\frac{\pi x}{a} \sin\frac{2\pi y}{l}$$

in all plate components, and two concave flanges are accompanied by two convex webs in the first half of length ($y \le l/2$).

The residual stresses are $\sigma_{yo}=\sigma_Y$ within the width $3t$=3.0cm on both sides of each corner and $\sigma_{yo}=-(3t/0.5a\text{-}3t)\sigma_Y$ in the rest areas.

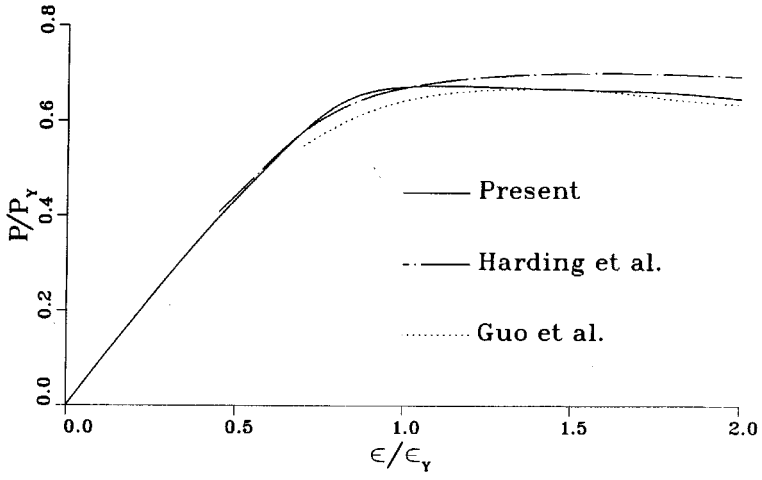

Fig. 3 Rectangular plate under compression

By virtue of symmetry, half of the box is analyzed using 16 strips of widths similar to those in the previous example. Six longitudinal series terms are taken and each strip is divided into three layers through the thickness direction. Further refined model only makes negligible difference.

As the end rotation β increases, the resulting bending moment M and the maximum deflection w_m of top flange are shown in Fig. 4. In this figure M_{cr}=1296 kN-m and β_{cr}=0.00292 radian are respectively the critical bending moment and corresponding end rotation, which are obtained from a finite strip stability analysis. The longitudinal profile of the buckling mode is identical to the geometrical imperfections. And M_p=1452 kN-m is the ultimate plastic moment obtained using beam theory.

As shown by this figure, while the end rotation is applied increasingly, the moment varies nonlinearly and the deflection increases constantly from the beginning because of the presence of the geometrical imperfections and the residual stresses. The bending moment reaches its maximum value M_u=0.872 M_{cr} at β=1.5 β_{cr} and then drops due to developing of plastic deformation in large areas.

5.3. Effect of the yield stress σ_Y

The above-mentioned structure is analyzed using the same model for different values of yield stress σ_Y. The level of residual stress is also modified proportionally but all other parameters remain unchanged. The resulting bending moment M vs end rotation β are depicted in Fig. 5 for σ_y=240 MPa, 320 MPa and 400 MPa, respectively. The results are also summarized in Table 1.

It can be noticed that the higher strength material shows lower bending moment at beginning because of the higher level of residual stress, and the ultimate bending moment M_u rises not as much as the yield stress σ_y increases.

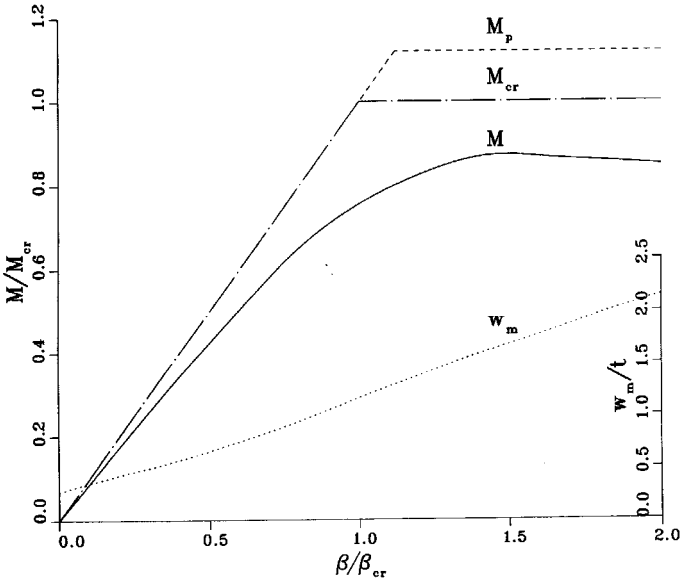

Fig. 4 Box beam under pure bending

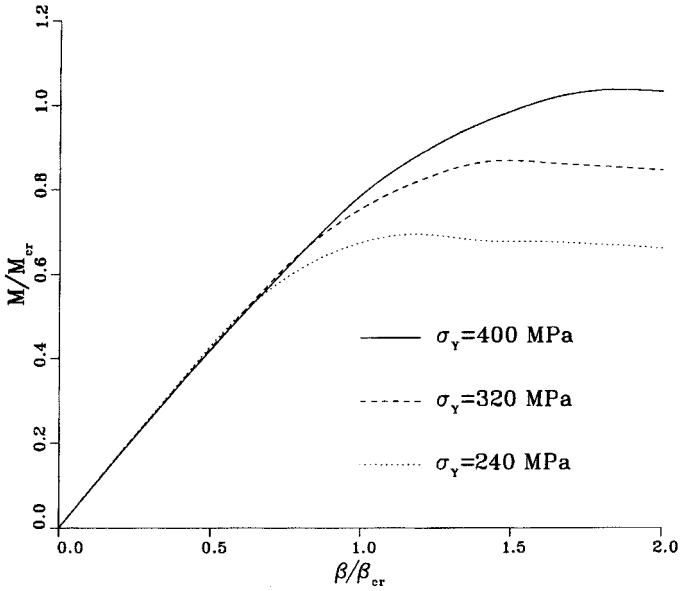

Fig. 5 Effect of yield stress

5.4. Effects of reduced residual stress and geometrical imperfections

Table 1 Effect of yield stress σ_Y

β/β_{cr}	M/M_{cr}		
	σ_Y=240 MPa	σ_Y=320 Mpa	σ_Y=400 MPa
0.5	0.429	0.425	0.421
1.0	0.675	0.755	0.787
1.2	0.695	0.824	0.888
1.5	0.678	0.872	0.988
1.8	0.671	0.858	1.039
2.0	0.662	0.848	1.035
M_p/M_{cr}	0.840	1.120	1.400
M_u/M_p	0.827	0.779	0.742

The structure in the second example is analyzed using the same model. However, the residual stresses are set to be zero with all other parameters unchanged. The results are listed in Table 2.

Then, the process is repeated with the geometrical imperfections reduced to

$$w_o = 0.001a \sin\frac{\pi x}{a} \sin\frac{2\pi y}{l}$$

and all other parameters identical to example 2. The results are also listed in Table 2. It can be seen that both changes enhance the strength and reduce the deflection at lower β, and the effect of reduced geometrical imperfections is more significant than zero residual stress.

Table 2 Effects of zero σ_{yo} and reduced w_o

β/β_{cr}	M/M_{cr}			w/t		
	Example 2	zero σ_{yo}	low w_o	Example 2	zero σ_{yo}	low w_o
0.4	0.343	0.383	0.371	0.572	0.485	0.166
0.8	0.652	0.734	0.702	0.942	0.851	0.624
1.0	0.755	0.844	0.808	1.163	1.103	0.940
1.2	0.824	0.881	0.873	1.376	1.362	1.206
1.4	0.867	0.889	0.904	1.583	1.585	1.407
1.5	0.872	0.886	0.911	1.686	1.685	1.502
1.6	0.867	0.883	0.913	1.769	1.780	1.599
1.8	0.858	0.875	0.907	1.970	1.959	1.794
2.0	0.848	0.866	0.898	2.152	2.125	1.974

6. Conclusions

In the present study, the finite strip method is successfully extended to the elasto-plastic postbuckling analysis of thin-walled structures under pure bending. This method is efficient and very convenient for parametric study.

Acknowledgements

The financial supports from the Department of National Defence and the Natural Sciences and Engineering Research Council of Canada are gratefully acknowledged.

References

Cheung, M.S., Li, W. and Chidiac, S.E. (1996), *Finite Strip Analysis of Bridges*, E and FN SPON, London.

Guo, Y.L. and Lindner, J. (1993), "Analysis of elastic-plastic interaction buckling of stiffened panels by spline finite strip method", *Computers and Structures*, **46**(3), 529-536.

Hancock, G.J. (1981), "Nonlinear analysis of thin sections in compression", *Journal of Structural Division, Proc. ASCE*, **107**(ST3), 455-471.

Harding, J.E., Hobbs, R.E. and Neal, B.G. (1977), "The elasto-plastic analysis of imperfect square plates under in-plane loading", *Proc. Inst. Civil Engrs, Part 2,* **63**, 137-158.

Owen, D.R.J. and Hinton, E. (1980), *Finite Element in Plasticity* (Theory and Practice), Pineridge Press, Swansea.

Sridharan, S. and Graves-Smith, T.R. (1981), "Postbuckling analyses with finite strips", *Journal of Engineering Mechanics Division, Proc. ASCE*, **107**(EM5), 869-888.

Zienkiewicz, O.C. (1977), *The Finite Element Method*, third edt., McGRAW-HILL, London.